A Flexible Inkjet-Printed Memristive Sensor: Modeling and Simulation

[†]Tasnim Zaman Adry, [‡]Steven D. Gardner, [†]Sazia Afreen Eliza, and [†]Mohammad Rafiqul Haider
[†]*Dept. of EECS, University of Missouri-Columbia (MIZZOU)*
Columbia, MO, USA
{mhaider}@missouri.edu
[‡]*EITD, University of Alabama at Birmingham (UAB)*
Birmingham, AL, USA

***Abstract*—The exploration of neuromorphic computing, driven by the demand for efficient data-intensive operations, relies on memristive devices for versatile information storage. In this study, a low-cost, nonlinear, current-controlled memristor using hexagonal boron nitride (hBN) and graphene inkjet-printed materials is proposed for neuromorphic computing applications. The memristor device, designed with a standard office piezoelectric printer, demonstrates the feasibility of inkjet printing technology for flexible and cost-effective computing solutions. The research investigates the use of nanoparticle-based inks and explores the potential of inkjet-printed circuits as an eco-friendly and power-efficient alternative. An empirical model is developed using MATLAB to analyze the behavior of the inkjet-printed memristor device, with insights complemented by a physical Simscape model. This work contributes to the advancement of flexible and low-cost memristor devices, facilitating their integration into neuromorphic computing architectures and other applications requiring versatile information storage.**

***Index Terms*—Neuromorphic computing, Memristors, MATLAB modeling, Inkjet printing, Flexible Electronics**

I. Introduction

Memristors, initially predicted by Leon Chua in 1971, have garnered significant attention in recent years due to their potential to revolutionize computing systems, particularly in the realm of neuromorphic computing [1]. Because of its two-terminal design, ultra-low power, ease of fabrication, low cost of manufacturing, appropriateness for synaptic computing, and ability to store data at extremely high densities, memristors provide a number of benefits [2]. Neuromorphic algorithms, renowned for their prowess in vision, speech, and intelligent processing, often demand substantial memory and computing resources [3]. However, it has become more and more difficult to achieve substantial power efficiency gains through the scaling down of traditional CMOS technique, and the "memory wall" bottleneck affects the efficiency of von Neumann architecture [4]. Memristor-based computation offers a promising avenue to enhance power efficiency in neuromorphic computing systems, yet the absence of a behavior-level simulator poses a significant challenge.

Since their experimental demonstration by HP Labs in 2008, memristors have evolved into a critical component for large-scale neuromorphic systems [5]. The applied voltage/current pulse controls the device's non-linear switching behavior in resistance values, which varies in response to changes in charge flow across the device [6]. These thin-film devices, capable of remembering total electric charge/flux flow, boast impressive integration densities of up to 100 Gb/cm2, making them ideal for memory-intensive applications [7]. It is a promising tool for massively parallel, large-scale neuromorphic systems because of these special qualities [8].

The majority of memristor research to date has been done with thin film processing methods that work well with the creation of high-density memory. This might not be the best solution for the subject of flexible electronics, though. Compared to other methods like screen printing, inkjet printing enables for the quick deposition of extremely small ink volumes (picolitres), which achieves excellent pattern accuracy and resolution with improved repeatability. This makes it a particularly promising technology for fabricating memristor devices on flexible substrates [9], [10].

Recent advancements in organic and hybrid composite materials have further fueled interest in printed electronics, offering new opportunities for flexible devices in diverse applications such as wearable technologies, health monitoring, and prosthetics [11]–[13]. There is increasing demand for electronic devices that can be used in a variety of non-conventional environments and applications, which traditionally would not be considered appropriate for fragile and expensive semiconductors devices that are susceptible to easy breakage or damage from the elements. Memristors, as a form of non-volatile memory, present several advantages including low power consumption, simplicity, and cost-effective manufacturing. Several studies have proposed completely printed flexible MoS2 memristive artificial synapses [14], inkjet-printed h-BN memristors for hardware security [15], aerosol jet-printed WSe2 crossbar architecture devices on Kapton [16], and printed memory devices using various nanomaterials [17], [18]. However, there is a lack of thorough study on the formation and propagation of filament in randomly built networks of nanosheets created by printing processes, which results in limited durability and poor repeatability of the device.

This paper aims to address these challenges by proposing an inkjet-printed, low-cost flexible memristor device, exhibiting

This work was supported by the USA National Science Foundation under Grant No. ECCS-2201447.

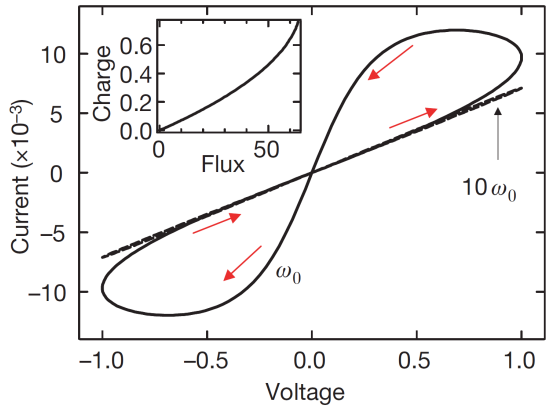

Fig. 1: I-V characteristic of HP memristor model [5]

the characteristic I-V curve of a pinched hysteresis loop inherent to memristor devices. We utilize MATLAB Cftool to develop an empirical model that accurately fits our experimental results. Additionally, we present a Simulink model and a Simscape model for the physical deployment of our device, paving the way for the development of reservoir networks.

II. Memristor Fundamentals

Resistance transition properties of memristive devices, which are typically MIM sandwich structures, are intimately related to their electrodes and switching materials [19]. Pinched hysteresis loops and state variables dictate memristors. Spin memristors, phase-change memristors, thermistors, and ion channels in neurons are examples of generalized memristors.

Fig. 1 shows the I-V characteristic of the first physical memristor, a bipolar TiO2 thin film, developed by HP labs in 2008 [5]. Since then the pinched hysteresis loop became a characteristic of memristors, when experimental evidence demonstrated this behavior in memristive devices. This pinched region indicates a distinct behavior where the resistance of the memristor changes abruptly in response to changes in voltage or current.

Formally, a current-controlled time-invariant memristive system is represented by

$$\frac{d\omega}{dt} = f(\omega, i) \tag{1}$$

$$v(t) = R(\omega, i)i(t) \tag{2}$$

Technical difficulties with memristor-based memory include creating a read circuit for the memristor state, resolving the stability of its resistive state during the read process, and acquiring experimental data for actual memristor structures. A thorough analysis of memristor-based memory is still absent.

The total resistance of a memristor is the sum of the resistances in the doped and undoped regions.

$$R_{MEM}(x) = R_{ON}x + R_{OFF}(1 - x) \tag{3}$$

where R_{ON} and R_{OFF} are the memristor resistance limit values for $\omega = D$ and $\omega = 0$, and $x = \frac{\omega}{D}$ is the width of the

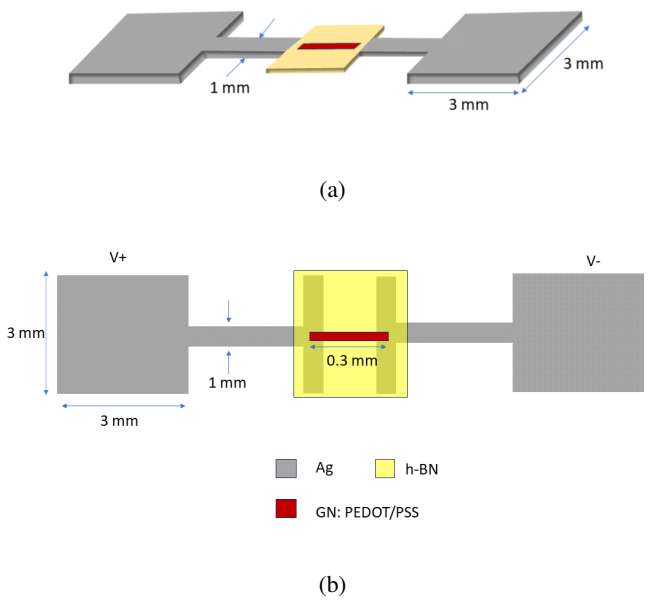

Fig. 2: Schematic of the inkjet-printed (iJP) memristor device. (a) 3D view of the iJP memristor device, and (b) Top view of the iJP memristor device with device dimensions.

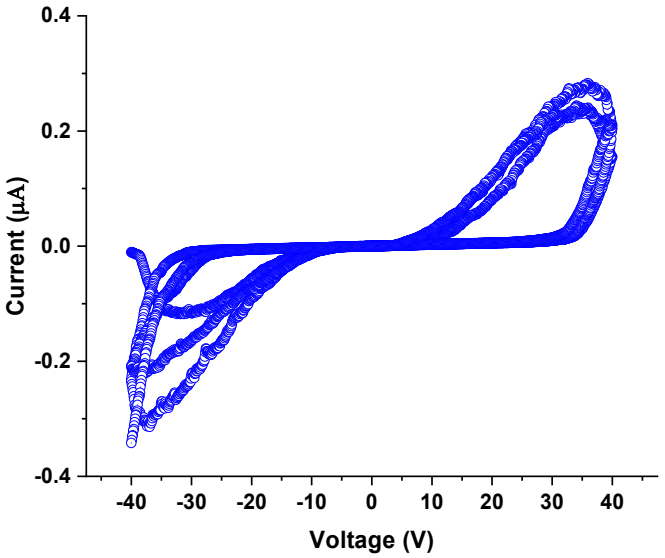

Fig. 3: Measured I-V characteristic of the iJP Memristor device. A Complete pinched-hysteresis loop is seen.

doped area, referred to the overall length D of the oxide layer. Typically, the two resistances' ratio is $10^2 - 10^3$. Ohm's law may be used to express the relationship between the memristor voltage and current:

$$v(t) = R_{MEM}(\omega)i(t) \tag{4}$$

The state equation states that the speed at which the border between the doped and undoped areas moves is dependent on

a number of factors, including the resistance of the doped area and the passing current.

$$\frac{dx}{dt} = Ki(t)f(x), K = \frac{u_v R_{ON}}{D^2} \tag{5}$$

Where u is the dopant mobility. Large electric fields may be produced by tiny voltages in nanoscale devices, which can lead to nonlinearities in the ion transport process. These nonlinearities are particularly pronounced at the thin film borders, where the speed of the boundary approaches zero.

III. Structural Design and Fabrication

The study explores the use of inkjet printing for the fabrication of a low-cost, nonlinear, voltage-controlled graphene memristor device, using matlab for numerical modeling. Inkjet printed (iJP) circuits may be used in nonuniform situations such as curved or uneven surfaces, fabrics, and nonrigid items [11]. A schematic of the iJP Memristor is shown in Fig. 2.

Using an Epson XP-960 drop-on-demand piezoelectric printer, parallel plates of silver nanoparticles are printed onto PET film to create the memristor. Graphene (GN/PEDOT: PSS) nanoparticle semiconductor ink is used to bridge the channel region between the plates. It is carefully deposited using an electronic pipette.

The print process involves printing silver plates with a spacing of around 130 μm, aligning the gap with the print head's moving axis, and examining conductivity. After applying hexagonal boron nitride (hBN) to the channel area, it is cured for five minutes at 150 °C to solidify it. This material serves as an insulated canvas for managing the channel region.

The coffee-ring effect, a flaw in IJP technology, disrupts nanoparticle uniformity and variability in reliability. A new method involves cutting a well into the hBN layer, restricting GN ink's spread and interaction with silver parallel plates. The cutting process can be automated using a V-One PCB printer, and the GN ink is then dropped onto the well to avoid the coffee-ring effect.

TABLE I: List of Parameters

Parameters	Forward Pass	Backward Pass
$p1$	1.51×10^{-16}	-1.45×10^{-16}
$p2$	-1.04×10^{-15}	-1.02×10^{-15}
$p3$	-2.37×10^{-13}	1.82×10^{-13}
$p4$	4.7×10^{-12}	3.99×10^{-12}
$p5$	-3.57×10^{-11}	8.67×10^{-11}
$p6$	6.14×10^{-10}	1.43×10^{-9}
$p7$	1.51×10^{-10}	-1.43×10^{-10}

IV. I-V Characteristics

The iJP memristor device was analyzed for its memristive behavior, which is a memory effect that causes the I-V curve to have a loop rather than a single line. Memristors and Schmitt triggers are two excellent examples of hysteretic devices, with their output signal changing into many states depending on the signal's history. These devices exhibit high non-linearity with varying states and natural time-series characteristics, making them ideal candidates for use as reservoirs. The iJP memristors used the hBN and GN/PEDOT: PSS mixture as the semiconductor, which has a unique I-V curve. The iJP memristos's I-V curve accurately depicts the device's memristive activity as shown in Fig. 3. At the range of 30-40 V, the current jumps suddenly while the positive voltage increases gradually.

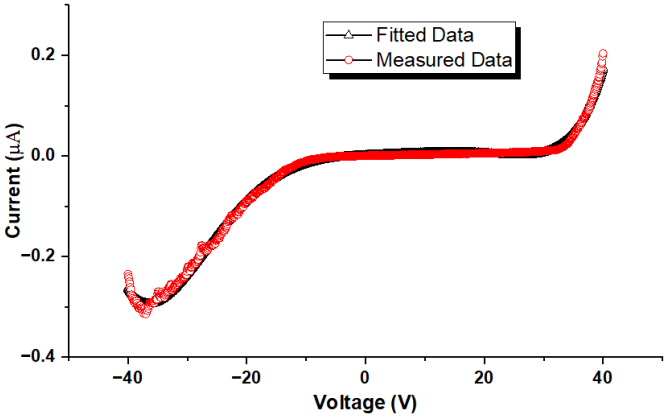

(a) Forward pass

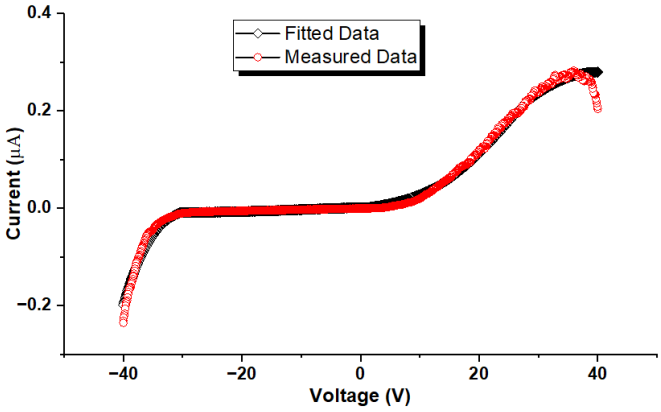

(b) Backward pass

Fig. 4: Curve fitting with the experimental results.

During the SET process, the device flips between the low resistance state (LRS) and the high resistance state (HRS), and between -30 and 40 volts, it goes back to the LRS. The signal exhibits notable non-linearity and a distinct hysteresis curve, which is more difficult to model for simulation studies due to intricate exponential regressions.

V. Memristor Modeling in Matlab

There are several memristor models have been reported in the literature. The Ion-Drift model, as explained in section II exhibits no-threshold conduction. A different model reported by Yakopcic [20] shows a threshold in the forward pass but no threshold in the backward pass. Unlike the previous two approaches, our iJP Meristor device shows thresholds in both forward and backward passes. Therefore, this study takes resorts of an empirical model using MATLAB CFtool to fit experimental results accurately. The model separates the I-V

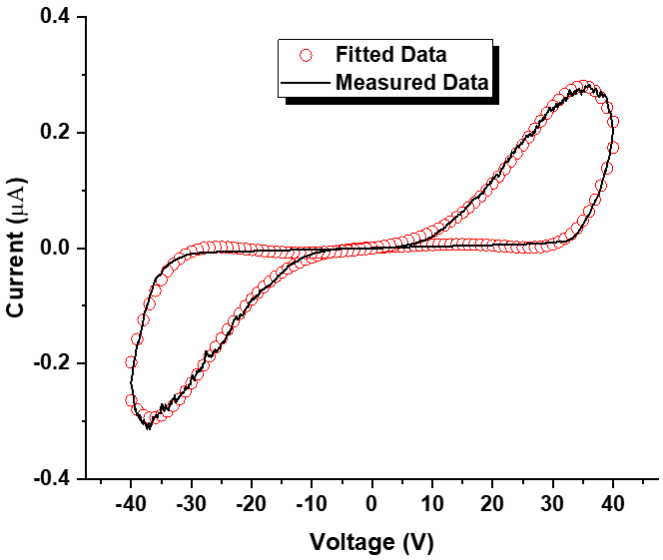

Fig. 5: I-V characteristic of the simulated iJP Memristor model.

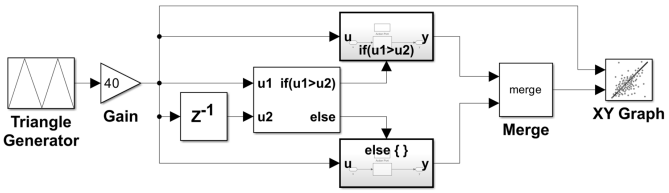

Fig. 6: Simulink model of the iJP Memristor.

curve into forward (-40V to 40V) and backward (40V to -40V) passes, generating distinct equations for each. These equations are then merged to form a perfect pinched hysteresis loop, represented by a 6^{th} order polynomial. The empirical equation can be shown as:

$$y = p1.x^6 + p2.x^5 + p3.x^4 + p4.x^3 + p5.x^2 + p6.x + p7 \quad (6)$$

The variable values $(p1, p2, p3, p4, p5, p6, p7)$ differ for forward and reverse passes, as detailed in Table I. The experimental curve and fitted curve is shown in Fig. 4. The practical aspect of memristor modeling in MATLAB is demonstrated, reproducing memristor behavior using empirical equations.

Simulation results for input voltages ranging from -40V to 40V are accurately depicted in Fig. 5. The simulation results match the experimental data with R^2-value of 0.9972 for forward pass and 0.9961 for backward pass. A Simulink environment is a better option when the memristor is to be modeled as an element of complex systems. Additionally, a Simulink model is developed based on the empirical equations, ensuring consistency with experimental results as shown in Fig. 6.

The Simulink environment also contains the Simscape block library intended for multidomain modeling of physical systems. We also developed a physical Simscape model that can be used in the future to build reservoir networks. The Simscape

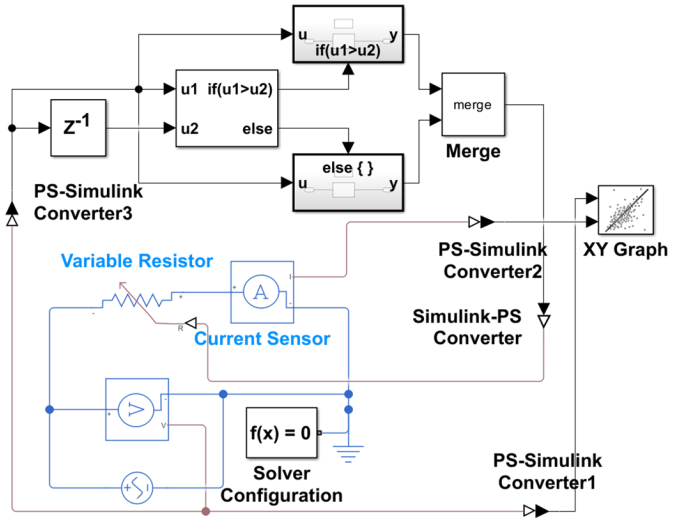

Fig. 7: Physical iJP memristor model in Simulink and Simscape.

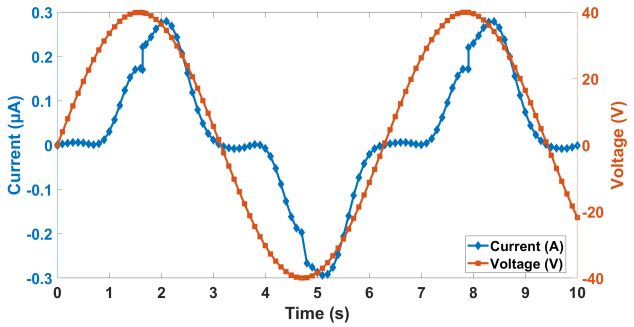

Fig. 8: Time response of the iJP Memristor showing the input sinusoidal voltage and the corresponding skewed output current due to the pinched hysteresis behaviour of the device.

model is shown in Fig. 7. The current output for the Simulink model for a sinusoidal input voltage is shown in Fig. 8. As is evident from Fig. 8, the current output is skewed due to the pinched hysteresis threshold voltages in both forward and backward conduction processes.

VI. Conclusion

In conclusion, this paper has presented a comprehensive study on the development and characterization of an inkjet-printed memristor device using hexagonal boron nitride (hBN) and graphene inkjet-printed materials. This memristor exhibits unique I-V characteristics, including pinched hysteresis loops, making it well-suited for memory tasks. The study has also introduced an empirical model developed using MATLAB Cftool, providing insights into the behavior of the memristor device. Additionally, Simulink and Simscape models have been presented for the physical deployment of the device, offering opportunities for future applications. The developed models and fabricated device pave the way for the development of efficient and scalable computing systems with

applications in artificial intelligence, machine learning, and the Internet of Things (IoT). Overall, this work demonstrates the potential of inkjet-printed memristor devices for enhancing the performance and efficiency of neuromorphic computing systems, opening up new avenues for research and innovation in the field.

ACKNOWLEDGMENT

This work was supported by the USA National Science Foundation (NSF) under Grant No. ECCS-2201447. Any opinions, findings, and conclusions or recommendations expressed in this material are those of the author(s) and do not necessarily reflect the views of the National Science Foundation.

REFERENCES

[1] Chua L O 1971 Memristor-the missing circuit element IEEE Trans. Circuit Theory CT-18 507–19

[2] Jaafar, Ayoub H., Alex Gee, and N. T. Kemp. "Printed and flexible organic and inorganic memristor devices for non-volatile memory applications." Journal of Physics D: Applied Physics 56.50 (2023): 503002.

[3] Y. LeCun, Y. Bengio, and G. Hinton, "Deep learning," Nature, vol. 521, no. 7553, pp. 436–444, 2015.

[4] M. M. Waldrop, "The chips are down for Moore's law," Nature, vol. 530, no. 7589, pp. 144–147, 2016.

[5] D. B. Strukov, G. S. Snider, D. R. Stewart and R. S. Williams, Nature, 2008, 453, 80–83.

[6] Yoon, Kyung Jean, et al. "Electrically-generated memristor based on inkjet printed silver nanoparticles." Nanoscale Advances 1.8 (2019): 2990-2998.

[7] Y. Ho, G. M. Huang, and P. Li, "Nonvolatile memristor memory: Device characteristics and design implications," in Proc. IEEE/ACM ICCAD, Nov. 2009, pp. 485–490.

[8] Q. Xia, W. Robinett, M. W. Cumbie, N. Banerjee, T. J. Cardinali, J. J. Yang, et al., "Memristor-CMOS hybrid integrated circuits for reconfigurable logic," Nano Lett., vol. 9, no. 10, pp. 3640–3645, Sep. 2009.

[9] S. T. Han, Y. Zhou and V. Roy, Adv. Mater., 2013, 25, 5425–5449.

[10] Gardner, Steven D., et al. "Aluminum-doped zinc oxide (zno) inkjet-printed piezoelectric array for pressure gradient mapping." 2019 IEEE 62nd International Midwest Symposium on Circuits and Systems (MWSCAS). IEEE, 2019.

[11] Gardner, Steven D., and Mohammad R. Haider. "An inkjet-printed artificial neuron for physical reservoir computing." IEEE Journal on Flexible Electronics 1.3 (2022): 185-193.

[12] Gao, Meng, Lihong Li, and Yanlin Song. "Inkjet printing wearable electronic devices." Journal of Materials Chemistry C 5.12 (2017): 2971-2993.

[13] Yamada, Kentaro, et al. "Paper-based inkjet-printed microfluidic analytical devices." Angewandte Chemie International Edition 54.18 (2015): 5294-5310.

[14] X. Feng, Y. Li, L. Wang, S. Chen, Z. G. Yu, W. C. Tan, N. Macadam, G. Hu, L. Huang, L. Chen, X. Gong, D. Chi, T. Hasan, A. V. Thean, Y. Zhang and K. Ang, Adv. Electron. Mater., 2019, 5, 1900740

[15] K. Zhu, G. Vescio, S. González-Torres, J. López-Vidrier, J. L. Frieiro, S. Pazos, X. Jing, X. Gao, S. D. Wang, J. Ascorbe-Muruzábal, J. A. Ruiz-Fuentes, A. Cirera, B. Garrido and M. Lanza, Nanoscale, 2023, 15, 9985

[16] Y. Li, X. Feng, M. Sivan, J. F. Leong, B. Tang, X. Wang, J. N. Tey, J. Wei, K. W. Ang and A. V. Y. Thean, IEEE Sens. J., 2020, 20, 4653

[17] K. H. Choi, M. Mustafa, K. Rahman, B. K. Jeong and Y. H. Doh, Appl. Phys. A: Mater. Sci. Process., 2012, 106, 165

[18] N. M. Muhammad, N. Duraisamy, K. Rahman, H. W. Dang, J. Jo and K. Y. Choi, Curr. Appl. Phys., 2013, 13, 90

[19] Gao, Lili, et al. "Memristor modeling: challenges in theories, simulations, and device variability." Journal of Materials Chemistry C 9.47 (2021): 16859-16884.

[20] Yakopcic, Chris, et al. "Memristor model optimization based on parameter extraction from device characterization data." IEEE Transactions on Computer-Aided Design of Integrated Circuits and Systems 39.5 (2019): 1084-1095.